Preprint

20020064893
574485
276

Ab Initio and Improved Empirical Potentials for the Calculation of the Anharmonic Vibrational States and Intramolecular Mode Coupling of N-Methylacetamide

Susan K. Gregurick

Department of Chemistry and Biochemistry
University of Maryland, Baltimore County
1000 Hilltop Circle, Baltimore MD 20215

Galina M. Chaban[†], and R. Benny Gerber[‡]

[†]NASA Ames Research Center
Mail Stop 230-3, Moffett Field, CA 94035-1000

[‡]Department of Physical Chemistry and the Fritz Haber Research Center
The Hebrew University, Jerusalem 91904, Israel
Department of Chemistry
University of California, Irvine, California 92697

Abstract

The second-order Møller-Plesset *ab initio* electronic structure method is used to compute points for the anharmonic mode-coupled potential energy surface of *N*-methylacetamide (NMA) in the $trans_{ct}$ configuration, including all degrees of freedom. The vibrational states and the spectroscopy are directly computed from this potential surface using the Correlation Corrected Vibrational Self-Consistent Field (CC-VSCF) method. The results are compared with CC-VSCF calculations using both the standard and improved empirical Amber-like force fields and available low temperature experimental matrix data. Analysis of our calculated spectroscopic results show that: (1). The excellent agreement between the *ab initio* CC-VSCF calculated frequencies and the experimental data suggest that the computed anharmonic potentials for *N*-methylacetamide are of a very high quality. (2). For most transitions, the vibrational frequencies obtained from the *ab initio* CC-VSCF method are superior to those obtained using the empirical CC-VSCF methods, when compared with experimental data. However, the improved empirical force field yields better agreement with the experimental frequencies as compared with a standard AMBER-type force field. (3) The empirical force field in particular overestimates anharmonic couplings for the amide II mode, the methyl asymmetric bending modes, the out-of-plane methyl bending modes, and the methyl distortions. (4) Disagreement between the *ab initio* and empirical anharmonic couplings is greater than the disagreement between the frequencies, and thus the anharmonic part of the empirical potential seems to be less accurate than the harmonic contribution. (5) Both the empirical and *ab initio* CC-VSCF calculations predict a negligible anharmonic coupling between the amide I and other internal modes. The implication of this is that the intramolecular energy flow between the amide I and the other internal modes may be smaller than anticipated. These results may have important implications for the anharmonic force fields of peptides, for which *N*-methylacetamide is a model.

I. Introduction

There is long standing interest in the spectroscopy and dynamics of *N*-methylacetamide (NMA). This is due in part because NMA can serve as a simple model for the amide bond in peptides and proteins. The importance of the amide group lies in it's contribution to both intramolecular backbone hydrogen bonding and solvent-protein hydrogen bonding. An experimental estimate for the energetics of main chain hydrogen bonding is between $1.3 +/- 0.6$ and $1.5 +/- 0.3$ $kcal/mol$.[1,2] In order to accurately represent the physics of the amide bond, it is important to first understand both the intramolecular forces and the coupling this amide group undergoes. This implies a detailed investigation of the molecular forced fields used for *N*-methylacetamide, from both an empirical and an *ab initio* perspective. However, any such study should not only include the energetics of the different conformers of NMA, but also anharmonic vibrational spectroscopy and the effects of intramolecular vibrational mode coupling. One interesting example of amide coupling may be illustrated in the two broad subbands found in the vibrational Raman spectrum for the amide I mode of NMA in H_2O.[3] In this work, Chen *et. al* found that these two subbands were probably not due to different conformations of the NMA, but could in fact be attributed to coupling between the amide I mode to the bending mode of the solvent H_2O molecules. However, in the femtosecond IR pump-probe spectra of NMAD (Deutrated NMA) Hamm and co-workers found the same doublet structure in the amide I band for NMAD in D_2O and suggested that this subband could not be due to coupling to the OD bending mode of D_2O.[4] Along a similar line of work, Pajcini and Asher investigated excitonically coupled states which mix the primary and secondary amide transition of *N*-acetylglycinamide (NAGA).[5] By looking at the polarized-oriented Raman spectra of single crystal NAGA, they were able to show that the primary and secondary amide III and amide I vibrations are excitonically coupled. Therefore it is still an open question if the coupling of the amide I mode is to other internal modes or to the solvent modes. The question of intra/intermolecular mode coupling becomes even more important when considering vibrational energy redistribution pathways as measured by femtosecond nonlinear-infrared spectroscopy.[4]

Notwithstanding the deep and detailed experimental[6–13,3,14,6] and theoretical[15–22] investigations of *N*-methylacetamide, relatively little is still known about the intramolecular coupling between different vibrational modes and the effect of this on spectroscopy. In previous *ab initio* theoretical calculations of the energetics and harmonic vibrational spectra of *N*-methylacetamide, it was illustrated that one needs to scale the harmonic frequencies to reasonably compare with the experimental data.[16] In addition, the different conformations of NMA (*cis* and *trans*) require slightly different scaling factors. Furthermore, when the amide group is hydrogen bonded to water, this also requires rescaling of the force constants.[16] Thus, although the *ab initio* theoretical calculations of *N*-methylacetamide were of a reasonable level, the calculated harmonic vibrational frequencies required scaling in order to compare well with known experimental data.[16,22,17,21,18] Because scaling is an empirical and non-transferable procedure, vital information regarding the spectroscopy and more importantly the anharmonic nature of the underlying molecular force field, is lost. Therefore, it is beneficial to derive an *ab initio* molecular force field that will not only directly reproduce the vibrational spectroscopy but also the anharmonic intramolecular mode coupling nature of the molecule.

One can, in principle, measure vibrational frequencies quite accurately with low temperature vibrational spectroscopy, either in rare gas matrices,[23] in a nozzle jet expansion,[24–29] or in

He droplets.[30–32] This is because at lower temperatures the effects of line broadening and frequency shifting will be minimized. For example, in the recent superfluid He droplet experiments of Huisken *et. al*, the authors could spectroscopically resolve different conformers of glycine based on the OH stretching frequency. When the OH in glycine is internally hydrogen bonded, the frequency will be red shifted by 300 cm^{-1}.[23] Furthermore, recent developments in the field of two-dimensional infrared spectroscopy show substantial promise in the ability to not only ascertain anharmonic shifts in vibrational frequencies, but also to resolve mode-coupling effects.[33,34,4,35–38] This newly emerging experimental field requires a companion in the theoretical understanding of anharmonic mode-coupled vibrational spectroscopy which we shall begin to address by employing the Correlation Corrected Vibrational Self-Consistent Field method.

When the potential is available in an analytical form, one can perform a Vibrational Self-Consistent Field (VSCF) calculation in order to determine the frequencies and relative degree of mode coupling in the system. This has proven to be quite accurate and useful for a wide variety of problems such as $(Ar)_{13}$ clusters,[39] peptide-water complexes,[40] glucose,[41] and BPTI with almost 200 hydration waters.[42] Moreover, by extending the VSCF method using perturbation-corrections treatments, Jung and Gerber were able to deal quite successfully with the highly anharmonic coupled mode system, $(H_2O)_n$, $n \leq 8$.[39] Obviously, this method is as successful as the underlying analytical force field is accurate. Until recently, only empirical force fields were used in the calculation of spectroscopy at an anharmonic level for all but very small molecules. Recently, Chaban *et al.* have developed an algorithm that combines anharmonic vibrational spectroscopy with direct calculation of *ab initio* potentials.[43] The method accounts for the anharmonicities and couplings between vibrational modes using the Correlation Corrected Vibrational Self-Consistent Field (CC-VSCF) approach and, therefore, provides a superior alternative to the existing techniques based on scaling the harmonic vibrational frequencies. This method does not require a fitting of an analytic potential function, nor high order derivatives. Thus, direct calculation of the anharmonic vibrational spectroscopy is feasible for molecules up to 15 atoms. The direct *ab initio* VSCF method was successfully applied to the calculation of the fundamental excitations of a number of hydrogen-bonded systems,[44] different conformers of glycine,[45] and a glycine-water complex.[46] It is our aim to apply this method for the calculation of the anharmonic vibrational spectrum of *trans* *N*-methylacetamide. In particular, we shall investigate the intramolecular mode coupling between different pairs of vibrational modes, as compared to the results obtained from a calculation of the anharmonic vibrational spectrum using an empirical force field. We shall be able to directly assign a coupling strength to each pair of modes. This work represents a continuing investigation into the nature of anharmonic coupling in biological molecules, and can be directly compared to experimentally determined two-dimensional vibrational spectrum.

The paper is organized as follows: A general discussion of the vibrational self consistent field method is given in section III. Section III, part A will outline the empirical force field and the empirical VSCF method, while part B will discuss the *ab initio* VSCF method and the energy calculations. The results and a discussion is given in section IV and the conclusions follow in section V.

II. Vibrational Self Consistent Field Method (VSCF) and Correlation-Corrected VSCF

Consider the vibrational Schrödinger equation:

$$[-\frac{\hbar^2}{2}\sum_{j=1}^{N}\frac{\partial^2}{\partial Q_j^2} + V(Q_1,...,Q_N)]\Psi(Q_1,...,Q_N) = E\Psi(Q_1,...,Q_N)$$

2.1

treated here in mass-weighted normal mode coordinates, where Q_j is the j^{th} mass-weighted normal mode coordinate and $V(Q_1;...,Q_N)$ is the full potential which includes anharmonicity and coupling between all of the modes. One may simplify equation 2.1 by utilizing the separable Hartree approximation, which is the basis of the VSCF method:[47-50]

$$\Psi(Q_1,...,Q_N) = \prod_{k=1}^{N}\psi_k^n(Q_k)$$

2.2

This then leads to N single mode VSCF equations of the following form:

$$[-\frac{\hbar^2}{2}\frac{\partial^2}{\partial Q_k^2} + V_k^n(Q_k) - \varepsilon_k]\psi_k^n(Q_k) = 0$$

2.3

where the effective potential for mode k is given by:

$$V_k^n(Q_k) = <\prod_{l\neq k}^{N}\psi_l^n(Q_l)|V(Q_1,...,Q_N)|\prod_{l\neq k}^{N}\psi_l^n(Q_l)>$$

2.4

Equations 2.3 and 2.4 for the single mode wavefunctions, energies, and effective potentials must be solved self-consistently. The VSCF expression for the total energy of vibrational state n is thus a sum of all the individual mode energies minus a term which accounts for the double counting of the interactions in the energy calculation and has the following form:

$$E_{total}^n = \sum_{k=1}^{N}\epsilon_k^n - (N-1) < \prod_{k=1}^{N}\psi_k^n|V(Q_1,...,Q_N)|\prod_{k=1}^{N}\psi_k^n >$$

2.5

In order to account for correlation effects between modes, an effective perturbation treatment analogous to Møller-Plesset method (MP2) for electronic structure calculations, is employed. In this treatment, the expression is up to second order perturbation in ΔV, and is as follows:

$$\Delta V(Q_1,...,Q_N) = V(Q_1,...,Q_N) - \sum_{k=1}^{N} V_k^n(Q_k).$$

2.6

The second-order correlation-corrected approximation for the energy is:

$$E_n^{cc} = E_n^{VSCF} + \sum_{m \neq n} \frac{| < \prod_{k=1}^{N} \Psi_k^n(Q_k) | \Delta V | \prod_{k=1}^{N} \Psi_k^m(Q_k) > |^2}{E_n^0 - E_m^0}.$$

2.7

In equation 2.7 we assume that there are no degenerate excited states (n,m), with energy $E_n^0 = E_m^0$. The theory behind the correlation-corrected VSCF (CC-VSCF) approximation can be found in references 39 and 43-49.

A. An Expansion Approach to the CC-VSCF Method and the Empirical Force Field

In the present study we utilized an empirical potential which is based on an Amber type of force field. Amber is one of the more widely used force fields in many biological studies./citeWeiner84,Weiner86 The functional form for the analytical potential is as follows:[51]

$$V(\vec{R}) = \sum_{bonds} K_r(r - r_{eq})^2 + \sum_{angles} K_\theta(\theta - \theta_{eq})^2 + \sum_{dihedrals} \frac{V_n}{2}[1 + cos(n\phi - \gamma)] +$$
$$\sum_{i<j}[\frac{A_{ij}}{R_{ij}^{12}} - \frac{B_{ij}}{R_{ij}^{6}} + \frac{q_i q_j}{\epsilon R_{ij}}] + \sum_{i<j}[v_{14}(\frac{A_{ij}}{R_{ij}^{12}} - \frac{B_{ij}}{R_{ij}^{6}}) + el_{14}\frac{q_i q_j}{\epsilon R_{ij}}]$$

2.A.1

Here $\vec{R}$ is a vector containing the x,y,z coordinates of all the atoms, r represents the norm of the bonding vector between any 2 connected atoms, and θ is the angle between any 3 bonded atoms. The dihedral angle, ϕ, includes both proper and improper torsion, where γ is a phase factor and V_n is the torsional barrier parameter. The last two terms in equation 2.A.1 represent the Van der Waals and electrostatic interactions, which are calculated between atoms of either different molecules, or on the same molecule but separated by at least 3 bonds ($v_{14} = 8$ and $el_{14} = 1.2$). Here R_{ij} is the distance between atoms i and j, $A_{ij}, B_{i,j}$ are the Van der Waals parameters, and q_i is the partial charge on atom i. This force field is based on the *ab initio* work of Cornell *et al.* and is adjusted to fit the experimental vibrational spectrum of *trans N*-methylacetamide.[13,16] This was accomplished by binning both the torsional parameters as well as the partial charges on the methyl group atoms. A Monte Carlo search was performed on the adjustable parameters, in conjuction with a VSCF calculation of the vibrational frequencies, in order to reach better agreement with the experimental data. The best fit molecular parameters for the implementation of the improved empirical force field can be found in Table I.

Assuming the system is not extremely anharmonic we can apply a power expansion about an equilibrium position to obtain the VSCF effective potential, $V_k(Q_k)$ of equation 2.4. Here $V_k(Q_k)$ is calculated by averaging over all the other $l \neq k$ modes as follows:

$$V_k(Q_k) = \frac{1}{2}\frac{\partial^2 V}{\partial Q_k^2}Q_k^2 + \frac{1}{6}\frac{\partial^3 V}{\partial Q_k^3}Q_k^3 + \frac{1}{24}\frac{\partial^4 V}{\partial Q_k^4}Q_k^4 + \frac{1}{2}\sum_{l\neq k}^{N}\frac{\partial^3 V}{\partial Q_k^2 Q_l}Q_k^2 < \psi_l(Q_l)|Q_l|\psi_l(Q_l) > +$$

$$\frac{1}{2}\sum_{l\neq k}^{N}\frac{\partial^3 V}{\partial Q_k Q_l^2}Q_k < \psi_l(Q_l)|Q_l^2|\psi_l(Q_l) > + \frac{1}{4}\sum_{l\neq k}^{N}\frac{\partial^4 V}{\partial Q_k^2 Q_l^2}Q_k^2 < \psi_l(Q_l)|Q_l^2|\psi_l(Q_l) >$$

2.A.2

Here, the effective potential is based on an expansion (Taylor Series) up to fourth order about a local/global minimum, however a grid-based method is also acceptable. In our present calculation we have neglected the cubic and higher order terms with non repeating indices ($Q_kQ_lQ_m, Q_kQ_lQ_mQ_n$) as they will be exceedingly small and in fact vanish in a perturbation treatment which uses the harmonic approximation as the unperturbed Hamiltonian.[52] For $n > 2$ the expansion coefficients, $\frac{\partial^n V}{\partial Q_k^n}$, were calculated using finite differences.[53] The quartic expansion (eq 2.A.2), suffices for such systems, if one studies low-lying vibrational states, and if the molecule is only moderately anharmonic. However, some systems do exhibit strong anharmonic effects, as illustrated for $(H_2O)_n$ clusters,[54] in which case the expansion method fails completely. For this system, a grid-based method is superior to an expansion-based method. In the case of NMA, numerical test indicated that the expansion method and the grid method were equivalent, however the grid based method requires less cpu time, and thus was chosen.

In our present calculation, we solved each k VSCF Hamiltonian (eq. 2.3) using the collocation method of Yang and Peet.[55] For an adjustable grid, sensitive to each mode, we choose to work in the dimensionless variable, $\bar{q_k}$, where

$$\bar{q_k} = \frac{Q_k}{(\lambda_k)^{\frac{1}{4}}}.$$

2.A.3

Here λ_k is the $k-th$ eigenvalue of the Hessian. Convergence was determined when $[\Delta\sum_k[\varepsilon_k]] \leq 0.0001 kcal/mol$ from one iteration to the next.

B. *Ab Initio* Vibrational Self-consistent field Method:

The calculation of the effective potential, equation 2.4, in an *ab initio* method will scale unfavorably (in cpu time) if one were to apply a Taylor Series expansion about a given configuration. However numerical test indicated that the pair-interaction approximation used in the *ab initio* calculation, and the expansion method (equation 2.A.2) used for the empirical force fields, were nearly equivalent. Therefore, the approach taken was to assume that the potential function can be well represented by including interactions between only pairs of modes, and calculating the *ab initio*

potential on a two-dimensional grid.[39,54] Our experience with this approximation, which neglects direct coupling between triplets of normal modes, has been very encouraging.[43–45] In this pair-wise coupling approximation, the effective potential becomes:

$$V_{VSCF}(Q_1,...,Q_N) = \sum_{j=1}^{N} V_j(Q_j) + \sum_{i<j} V_{ij}(Q_i,Q_j)$$

2.B.1

where

$$V_j(Q_j) = V(Q_1 = 0,...,Q_j,...Q_N = 0)$$

and

$$V_{ij}(Q_i,Q_j) = V(Q_1 = 0,...Q_i,Q_j,...,Q_N = 0).$$

2.B.2

We stress that our numerical test for several biological molecules have shown that the pairwise approximation seems valid for such molecules, and that adding additional mode-couplings does not make a significant contribution in terms of the calculated frequencies.

An electronic structure calculation is first used to calculate the equilibrium configuration. Then from diagonalization of the Hessian at this configuration, the normal mode coordinates are obtained. In order to calculate the potential at each normal mode point, a transformation back to Cartesian coordinates is made, and the potential energy is then calculated at this displaced geometry. The diagonal and mode-mode pair-coupling potentials of equation 2.B.2 were calculated on a 8-point and $8X8$ grid which were later interpolated to a 16-point and $16X16$ grid.

Finally, the IR intensities are calculated using the dipole moment estimated along the normal coordinate the VSCF wavefunctions for the ground and excited vibrational states as:[44]

$$I_i = \frac{8\pi^3 N_A}{3hc}\omega_i| < \Psi_i^0(Q_i)|\vec{\mu}(Q_i)|\Psi_i^1(Q_i) > |^2.$$

2.B.3

In equation 2.B.3, ω_i is the CC-VSCF vibrational frequency for mode i and $\Psi_i^0(Q_i)$, $\Psi_i^1(Q_i)$ are the ground and excited state VSCF wavefunctions.

All *ab initio* calculations were performed using the GAMESS electronic structure program,[56] with second-order Møller-Plesset perturbation theory (MP2). The basis set used was a Dunning-Hay double zeta + polarization (DZP).[57] This level of theory was found to give satisfactory results for previous *ab initio*-VSCF calculations on small biological molecules: glycine,[44] and a glycine-water complex.[46] The number of *ab initio* single-point energy calculations required for both the diagonal and pair-coupling potentials is:

$$N_{points} = N_{mode}N_{grid} + \frac{N_{mode}(N_{mode}-1)}{2}N_{grid}^2$$

where N_{mode} is the number of normal modes, which in this case is 30, and N_{grid} is the number of grid points in one dimension. For the present calculation the number of points, on an 8-point grid, is 28,080. The total *ab initio* VSCF calculation required approximately 4 months of CPU time on a Octane SGI workstation.

III. Results and Discussion

In this work, anharmonic vibrational states and frequencies of *N*-methylacetamide were obtained for three potentials; a standard AMBER force field, an improved empirical force field calculated to agree with existing vibrational frequencies of this system, and the MP2/DZP *ab initio* anharmonic potential energy surface. For each of these potentials the first step involved computing the equilibrium structure. The starting structure was found from a simulated annealing simulation of the isolated N-methylacetamide using our modified empirical force field (Table 1). In this case the starting temperature of 300 K was slowly decreased to 5 K during the course of a 15 ps dynamics run with a time step of 15 fs. The resulting low energy structure ($trans - NMA_{cc}$) was further minimized using a steepest descents method until the norm of the forces were $\leq$ 0.0001. Other conformers of NMA were found by an adiabatic mapping of the rotation of the CO and NH methyl groups. In the previous *ab initio* calculations of Mirkin and Krimm, the lowest energy structure for *trans*-N-Methylacetamide was found to be in a cis-cis configuration ($trans - NMA_{cc}$).[16,22] Here cis-cis refers to the orientation of the two methyl groups H atom in relation to the CO and NH groups. Previous *ab initio* calculations of Mirkin and Krimm found a 0.01 $kcal/mol$ energy difference between $trans - NMA_{cc}$ and $trans - NMA_{tc}$.[16,22] By adiabatically mapping the rotation of the CO methyl group and minimizing using the improved empirical force field, we find the barrier of rotation from cis-trans to cic-cis to be 0.23 $kcal/mol$. In a similar manner, the barrier of rotation from cis-cis to trans-cis was found to be 0.65 $kcal/mol$. The energy difference between the cis-cis and trans-cis structures is 0.18 $kcal/mol$. However, in the current *ab initio* calculations, we find that the lowest energy structure for $trans - NMA$ is in the *cis-trans* configuration (*trans*-NMA_{ct}), as illustrated in figure 1. The cis-cis configuration ($trans - NMA_{cc}$) was not a stable minimum in the current *ab initio* calculations and thus it was disregarded for the vibrational analysis. The calculated energy difference on the improved empirical surface between *cis* and *trans* NMA is 4.5 $kcal/mol$ in favor of the *trans* conformer. Ataka and co-workers measured an enthalpic difference between the *trans* and *cis* conformers to be 1.3 $kcal/mol$,[13] and previous *ab initio* results suggest an energy difference of 2.5 $kcal/mol$ between these two structures.[16] Our current *ab initio* calculations suggest an energy difference of 2.48 $kcal/mol$, in complete agreement with the previous *ab initio* calculations of Mirkin and Krimm.[16,15,22] One reason why the empirical Amber-like force field could overestimate the energy difference between *cis* and *trans*-NMA is a lack of accuracy in the description of intramolecular hydrogen bonding present in the *cis* conformer.

Due to the length of time required to calculate the *ab initio* VSCF potential energy surfaces, we only calculated the anharmonic vibrational frequencies for the $trans - NMA_{ct}$ configuration (Figure 1). The original empirical CC-VSCF, adjusted empirical CC-VSCF, *ab initio* CC-VSCF, and the observed matrix isolated experimental frequencies are compared in Table 2, while the harmonic frequencies for all calculations are given in Table 3. The frequency assignments are also

given in Tables 2 and 3. The experimental frequencies were obtained in a low temperature nitrogen matrix (20K) as reported by Ataka.[13] *It is important to mention that in the present calculation, the ab initio harmonic and CC-VSCF anharmonic frequencies are not scaled.* Indeed, the advantage of the CC-VSCF method is that the anharmonic corrections are calculated from the anharmonic part of the potential, which is their true physical origin, rather than by a "scaling" procedure, which is merely an empirical method based on experience from previous systems. We find the difference in the frequencies between the harmonic and CC-VSCF calculations to be as high as 300 cm^{-1} (Table 3). One can expect that, in general, an error in the *ab initio* CC-VSCF method will be on the order of 20 cm^{-1}, based on previous *ab initio* CC-VSCF calculations,[44-46] and a Density Functional calculation.[58] Thus the anharmonicities of the vibrational modes of N-Methylacetamide are quite large.

From Table 2 it is clear that the *ab initio* CC-VSCF method is far superior to both the original and adjusted empirical CC-VSCF calculations. This is particularly true in the case of the amide I, II and III modes (1700 to 1265 cm^{-1}), which are thought to play a role in intramolecular energy redistribution pathways. The improved empirical CC-VSCF calculated frequencies for the amide I, II and III are 1662, 1569 and 1183 cm^{-1} respectively. This is compared to the calculated *ab initio* CC-VSCF frequencies of 1751, 1547 and 1283 cm^{-1} and the experimental frequencies of 1708, 1511 and 1265 cm^{-1}. Both empirical force fields were originally derived for solvated peptide groups. In solution, the observed N-methylacetamide amide I, II and III frequencies shift to 1622, 1580 and 1315 cm^{-1}.[16] The empirical force fields studied in the present work have difficulty in reproducing matrix isolated NMA vibrational frequencies, particularly in this region. This represents a general shortcoming for most empirical force fields used to study high resolution vibrational spectroscopy, i.e. vibrational spectroscopy at a level where the anharmonic effects are significant. The fact that experimental data comes from spectroscopy in rare-gas matrices, introduces an element of uncertainty, since the matrix shift effects can be substantial. However, in a recent paper on glycine[46] spectroscopic calculations for *ab initio* and empirical potentials were compared with matrix experiments *AND* with experiments in superfluid He droplets (where the matrix effects are negligible). The superiority of the *ab initio* potential over the empirical potential was found to be even greater when the frequencies were compared with those of the superfluid He droplet experiment.

It is also clear from Table 3 that some vibrational modes of NMA are quite anharmonic, as seen by a comparison between the *ab initio* harmonic and *ab initio* CC-VSCF frequencies. This is particularly true for the stretching frequencies of the NH and methyl groups (3495 to 2900 cm^{-1}). Because neither the force constants nor frequencies are scaled in the present *ab initio* calculation, the CC-VSCF method has difficulty in reproducing some of the asymmetric and symmetric bending modes of the methyl groups (1529 to 1394 cm^{-1}). One possible way to improve the accuracy of the *ab initio* calculations is to use a triple-zeta + polarization basis set (TZP). However the *ab initio* CC-VSCF calculation does quite accurately captures the lower frequency modes corresponding to the in plane and out-of-plane bends and the methyl distortions ($< 900\ cm^{-1}$). In this region, the empirical expansion method (eq 2.A.2) becomes less reliable. While the adjusted empirical frequencies compare well with both the experimental and anharmonic *ab initio* frequencies for the CH_3 asymmetric and symmetric stretches (3000 to 2900 cm^{-1}), the force field is unable to accurately describe the the amide I, amide II and amide III frequencies (Table 2). This is however, the main strength of the current *ab initio* CC-VSCF method, the ability to quite accurately describe

the anharmonitices of the amide frequencies of a peptide, without resorting to scaling.

In order to investigate further the degree of anharmonicity in the amide modes, we have defined a scalar quantity, the *coupling strength* (CS), which will indicate the degree of mode-to-mode-coupling. Here the coupling strength (CS) for the $1 \leftarrow 0$ transition, is defined as:

$$CS_{ij}^{1\leftarrow 0} = (0.5) * \frac{< \Psi_i^0(Q_i)\Psi_j^1(Q_j)|V_{ij}|\Psi_i^0(Q_i)\Psi_j^0(Q_j) > + < \Psi_i^1(Q_i)\Psi_j^0(Q_j)|V_{ij}|\Psi_i^0(Q_i)\Psi_j^0(Q_j) >}{\hbar(\nu_j^0 - \nu_i^0)}$$

3.1

In equation 3.1 we divide by the frequency difference between the modes, since in cases of near-degeneracy, the effects of a given magnitude of coupling element are much greater. Ψ_i^0 and Ψ_i^1 represent the ground and first excited state wavefunctions for mode i. The wavefunctions are determined self-consistently using equation 2.3. In equation 3.1, V_{ij} is the coupling potential, defined by equation 2.B.2 (*ab initio*) and the off-diagonal terms of equation 2.A.2 (empirical). Tables 4 and 5 give the matrix elements for the coupling strength $CS_{ij}^{1\leftarrow 0}$ for both the adjusted empirical (Table 4) and *ab initio* (Table 5) coupling potentials. One would read a symmetric matrix element ($CS_{ij}^{1\leftarrow 0}$) as representing the coupling strength between modes i and j.

The largest coupling strength ($CS^{1\leftarrow 0}$ = 4.1) calculated using the *ab initio* coupling potential is between the NCH_3 asymmetric stretch and CH_3 asymmetric stretch (matrix element 2,5 Table 5). In the case of the empirical coupling potential, the degree of coupling between the NCH_3 asymmetric stretch and CH_3 asymmetric stretch is greatly reduced, even though the frequencies are nearly degenerate. This is illustrated in figure 2, which is a comparison between the mode-to-mode coupling potentials for both the *ab initio* and the improved empirical force fields. Each line in figure 2 represents the coupling potential at a different Q_j value for the CH_3 asymmetric stretching mode at a given value of Q_i for the NCH_3 asymmetric stretching mode. All normal mode coordinates (Q_i) are in a dimensionless variable as given by equation 2.A.3. It can be seen from figure 2 that the *ab initio* coupling potential is significantly larger than the empirical potential, and the *ab initio* frequencies of these two modes are almost degenerate (14 cm^{-1} difference). Thus the probability of energy transfer between the NCH_3 asymmetric stretch and CH_3 asymmetric stretch is quite large in the *ab initio* case, 4.1, vs 0.0 calculated from the adjusted empirical potential energy surface.

The most interesting finding of the present work is the fact that the amide I mode, at 1708 cm^{-1}, does not couple to other internal modes, as seen by the 8^{th} row in both coupling strength matrices (Tables 4 and 5). This is true for both the empirical and the *ab initio* coupling potentials. We believe that this is a significant finding. In the previous femtosecond nonlinear-infrared spectroscopic studies of Hamm and co-workers, the amide I mode of NMAD (deuterated NMA) was found to have a vibrational relaxation of 450 fs.[4] This is quite fast, and therefore it was postulated that the vibrational energy transfer was internal via an intramolecular energy redistribution (IVR) process. Transfer to the solvent should take more time and is expected to be on the order of 10-100 ps. Because Hamm and co-workers also saw similar relaxation rates for three small globular proteins, they concluded that this relaxation process is essentially the same for the amide I mode of all systems, and is an intrinsic property of the peptide group itself. They proposed that the possible candidate modes for energy transfer in NMAD could be the amide IV band at 628 cm^{-1}, the amide III mode at 965 cm^{-1} or the CO out-of-plane bend at 1044 cm^{-1}. We had originally thought

that the relaxation may be a $2 \leftarrow 0$ transfer to the amide III or possibly the amide IV band, as there is no appreciable intramolecular coupling for an amide I $1 \leftarrow 0$ transitions. The most likely reason for this is that the amide I frequency is not near-degenerate to any other intramolecular frequencies, and furthermore, the mode-to-mode coupling of amide I is not as strong as other calculated intramolecular couplings. Because the coupling strength is weighted by the frequency difference, this makes the probability of intramolecular vibrational energy transfer (from $1 \leftarrow 0$) unlikely for the amide I mode in NMA. However, we also calculate the $2 \leftarrow 0$ coupling element between that amide I and other intramolecular modes, and did not find any appreciable coupling to either the amide III or the amide IV. Thus, it is possible that the amide I relaxation is due to energy transfer to the solvent, or to energy transfer between modes which are not simply expressed in a pair-wise fashion. We are currently investigating this further. It therefore still remains unclear which modes the experimental vibrational energy of the this mode is transfered to in such a short amount of time (450 fs).

In the case of the amide II mode, however, there is the probability of vibrational energy transfer to the other internal modes. For the *ab initio* case there are two likely intramolecular modes to receive energy, the NCH_3 asymmetric bend and the CH_3 asymmetric bend (modes 10 and 11). The empirical force field also predicts that the amide II couples to the NCH_3 asymmetric bend and the CH_3 asymmetric bend, although with different probabilities. However, in the case of the empirical force field, we also find significant coupling between the amide II and NCH_3 symmetric bend-NC stretch (mode 14), CO out-of-plane bend, CCH_3 rocking (mode 19) and the CO out-of-plane bend (mode 21). Figures 3 and 4 illustrate the coupling potentials between the amide II and the CH_3 asymmetric bend and the NCH_3 symmetric bend-NC stretch modes (mode 9 coupling to modes 11 and 14 respectively). In figure 3 it is clear that both force fields couple amide II with the CH_3 asymmetric bend. Although the calculated empirical mode-coupled potential energy curves are quite a bit larger than the corresponding *ab initio* calculated mode-coupled potential energy curves, the coupling strength is larger in the *ab initio* case. This is most likely due to the near-degeneracy (energy separation of 6 cm^{-1}) of the modes compared with an energy separation of 104 cm^{-1} in the empirical calculation.

In figure 4 it is quite clear that the empirical coupling potential greatly overestimates the coupling between the amide II and the NCH_3 symmetric bend-NC stretch (modes 9 and 14). Similar coupling overestimations exist between the other two modes (9 and 19; 9 and 21) as well. In part, th strong coupling potentials to these three internal modes may explain why the empirical amide II frequency is blue shifted by 22 cm^{-1} from the *ab initio* frequency. If one were to simulate an intramolecular vibrational energy relaxation process (IVR) between the amide II and other internal vibrational modes using an empirical force field, the probability of an erroneous energy transfer would exist in this case. In comparison between the empirically calculated and the *ab initio* calculated coupling strength, we find that many mode-to-mode couplings are overestimated using the empirical force field. It is therefore quite important to compare the *ab initio* and empirical coupling strengths and coupling potentials, in order to accurately gauge possible IVR pathways.

IV. Conclusions

In this paper we address the issue of calculating anharmonic vibrational spectroscopy of small biological molecules using two different methods to express the coupling between vibrational modes. In section I we propose an improved empirical force field, fit to existing spectroscopic data, in order to refine the force constants defining the molecule of interest, namely N-methylacetamide (NMA). We also calculated the full 30-by-30 pair-wise mode-coupled potential energy surface of NMA using the GAMESS electronic structure program with second-order Møller-Plesset perturbation theory (MP2).[56] We then calculated the anharmonic vibrational spectrum of N-methylacetamide using a Correlation Corrected Vibrational Self-Consistent Field approach, with the effective potentials defined by either the empirical or the *ab initio* force fields. Because the resulting CC-VSCF *ab initio* frequencies do not need to be scaled, they can be compared directly to both the empirical CC-VSCF and the experimental frequencies (Table 2).

We find that overall the comparison between the empirical, improved empirical, *ab initio* and experimental frequencies is quite good. In general, however, the *ab initio* CC-VSCF method illustrates a significantly better agreement with the experimental data. This particularly true for the important and geometrically characteristic modes of amide I, II and III which are found at 1708, 1511 and 1265 cm^{-1}. In fact, most of the *ab initio* CC-VSCF vibrational modes are within 30 cm^{-1} of the experimental data, as compared to the improved empirical frequencies which may be off by as much as 80 cm^{-1}. A further comparison between the *ab initio* harmonic and full CC-VSCF calculated frequencies (Table 3) illustrates that most of the *ab initio* harmonic frequencies are significantly shifted from their anharmonic counterparts. Because the shift in frequency is much larger than the error of the *ab initio* calculation, this emphasizes the need to utilize a fully anharmonic, mode coupled method such as a CC-VSCF calculation when comparing to experimental vibrational data. All in all, these results suggest the use of *ab initio* rather than empirical potential functions, whenever feasible.

We further defined a scalar quantity, the coupling strength, in order to gauge the probability of vibrational energy transfer processes ($1 \leftarrow 0$ transition). By calculating the intramolecular coupling strength for both the *ab initio* and empirical force fields, we find a few surprising results. First, the amide I mode does not appear to couple to other internal vibrational modes via a $1 \leftarrow 0$ transition. Therefore, it is possible that the experimental results of Hamm and co-workers,[4] which suggest that an intrinsic property of the amide I mode is to very quickly (450 fs) transfer vibrational energy to other internal modes, must come from either coupling directly to the solvent or coupling to transitions of lower frequency modes. We also find that the coupling of the amide II mode to other internal modes is overestimated by the empirical force field, even if the force field is adjusted to fit spectroscopic data. This overestimation could in fact lead to the calculation of intramolecular energy redistribution (IVR) pathways for amide II which are incorrect. In general, we find that the empirical coupling strength is overestimated for many other modes ranging from amide II to amide V. Therefore, a comparison between the coupling strength calculated using an empirical and *ab initio* force fields is a first step in not only benchmarking empirical potentials, but also in later developing of biomolecular force fields. Based on this work, we suggest that for small biologically relevant molecules it may be better to utilize an *ab initio* derived potential energy surface for spectroscopic applications, as well as for quantitative treatment of intramolecular vibrational energy flow.

V. Acknowledgments.

We are very grateful to Drs. R. Schweitzer-Stenner and N. Wright for helpful discussions and careful reading of the manuscript. SKG acknowledges a postdoctoral fellowship from the Sloan Foundation and the Department of Energy. GMC acknowledges a Golda Meir postdoctoral fellowship at the Hebrew University. This work is supported in part by the US-Israel Binational Science Foundation (to RGB). The research at UC Irvine was supported by a grant from the Molecular and Cellular Biophysics Division of NSF (contract MCB-9982629, to RBG).

Table I: Molecular Mechanical Parameters

bond	K_r $kcal/(mol\mathring{A}^2)$	r_{eq} Å
Ca-H	340.0	1.09
C-Ca	317.0	1.522
C-O	570.0	1.229
C-N	490.0	1.335
N-H	434.0	1.01
N-Ca	337.0	1.449
Ca-H	340.0	1.09

Angle Parameters

angle	K_θ $kcal/(mol\ radian^2)$	θ_{eq} deg
CO-Ca-H	40.0	109.5
CO-NH-Ca	50.0	121.9
Ca-CO-OC	80.0	120.4
Ca-NH-HN	30.0	118.04
Ca-CO-NH	70.0	116.60
H-Ca-H	38.0	109.5
OC-CO-NH	80.0	122.9
CO-NH-HN	20.0	120.0
CO-Ca-H	40.0	109.5
CO-NH-Ca	50.0	121.90
Ca-CO-OC	80.0	120.4
H-Ca-NH	40.0	109.5
H-Ca-H	38.0	109.5
H-Ca-H	38.0	109.5

Table I continued: Torsional Parameters			
torsion	$V_n/2\ kcal/mol$	n, periodicity of torsion	γ deg
H-Ca-CO-OC	0.0	2	0.0
H-Ca-CO-NH	0.0	2	0.0
CO-NH-Ca-H	0.0	2	0.0
HN-NH-Ca-H	0.0	2	0.0
OC-CO-Ca-NH	0.1	3	180
OC-CO-NH-Ca	2.5	2	180
CO-Ca-OC-NH	2.5	2	180
OC-CO-NH-HN	2.0	1	0.0
CO-NH-Ca-H	0.0	2	90
NH-Ca-CO-OC	0.0	2	0.0
OC-CO-NH-HN	2.0	1	0.0

Improper Torsional		
torsion	$K_\phi\ kcal/(mol\ radians^2)$	ϕ_{eq} deg
CO-Ca-OC-NH	100.0	0.0
NH-CO-HN-Ca	45.0	0.0

Van der Waals Parameters		
atom type	R^*	
H	1.387	0.0157
Ca	1.908	0.1094
Ca	1.908	0.1904
CO	1.908	0.105
OC	1.6612	0.21
NH	1.824	0.17
HN	1.487	0.0157

Table 2 : Summary of CC-VSCF Frequencies for *trans* N-Methylacetamide

Empirical	Adjusted Empirical	Ab Initio	Obs. (Matrix)[13]	assignment
3309	3310	3523	3498	NH stretch
2986	2985	2993	2978	NCH_3 as
2985	2986	2985	3008	CCH_3 as
2985	2986	3014	3008	CH_3 as
2984	2985	2979	2973	CH_3 as
2872	2873	2939	2958	NCH_3 ss
2868	2869	2950	2915	CCH_3 ss
1676	1662	1751	1708	amide I
1598	1569	1547	1511	amide II
1466	1465	1566	1472	NCH_3 asy bend (ab)
1459	1459	1541	1446	CH_3 ab
1461	1461	1557	1432	CCH_3 ab
1453	1461	1515	1446	NCH_3 ab
1459	1454	1468	1419	NCH_3 sb NC s
1388	1371	1421	1370	CCH_3 ab
1231	1183	1283	1265	amide III
1143	1148	1214	1181	NH opb, CH_3r CNs
1042	1033	1184	1089	CN s CH_3r
1029	1031	1119	1037	CO opb CCH_3r
990	983	1083		CO opb CCH_3r
956	954	1022	990	CH_3r CC s CO opb
947	950	891	857	amide V CH_3r
799	789	643	658	CH_3r CO ipb
687	686	637	626	CCs CO opb
577	571	439	439	amide IV CH_3r
440	402	487	391	CO opb CCH_3r
302	281	299	279	CNC d CCN d
227	234	245		CNC d CCN d CCH_3d
372	381	266		NCH_3 d
398	398	166		CCH_3 d

s=stretch, as=asymeteric stretch, ss=symmetric stretch, d=distortion, r=rocking,ab=asymmetric bend, sb=symmetric bend, ipb= in-plane bend, opb=out-of-plane bend

Table 3 : Summary of Harmonic Frequencies for *trans* N-Methylacetamide

Empirical	Adjusted Empirical	Ab Initio	Obs. (Matrix)[13]	assign
3316	3316	3751	3498	NH stretch
2992	2992	3261	2978	NCH_3 as
2992	2992	3248	3008	CCH_3 as
2992	2992	3245	3008	CH_3 as
2991	2991	3225	2973	CH_3 as
2878	2878	3133	2958	NCH_3 ss
2875	2875	3124	2915	CCH_3 ss
1679	1666	1780	1708	amide I
1597	1567	1584	1511	amide II
1466	1464	1548	1472	NCH_3 asy bend (ab)
1457	1457	1526	1446	CH_3 ab
1453	1453	1520	1432	CCH_3 ab
1453	1453	1508	1446	NCH_3 ab
1447	1447	1484	1419	NCH_3 sb NC s
1380	1359	1438	1370	CCH_3 ab
1218	1169	1309	1265	amide III
1134	1132	1208	1181	NH opb, CH_3r CNs
1021	1010	1173	1089	CN s CH_3r
984	984	1133	1037	CO opb CCH_3r
968	952	1074		CO opb CCH_3r
927	922	1020	990	CH_3r CC s CO opb
903	903	890	857	amide V CH_3r
793	780	634	658	CH_3r CO ipb
661	659	624	626	CCs CO opb
575	570	428	439	amide IV CH_3r
438	399	362	391	CO opb CCH_3r
295	272	270	279	CNC d CCN d
217	219	153		CNC d CCN d CCH_3d
351	351	53		NCH_3 d
361	360	166		CCH_3 d

s=stretch, as=asymeteric stretch, ss=symmetric stretch, d=distortion, r=rocking,ab=asymmetric bend, sb=symmetric bend, ipb= in-plane bend, opb=out-of-plane bend

References

[1]B. A. Shirley, P. Stanssens, U. Hahn, and C. N. Pace, Biochemistry, **31**, 725 (1992).

[2]W. Lu, M. A. Qasim, M. Laskowski, and S. B. H. Kent, Biochemistry, **36**, 673 (1997).

[3]X. G. Chen, R. Schweitzer-Stenner, S. Krimm, N. G. Mirkin, and S. A. Asher, J. Am. Chem. Soc., **116**, 11141 (1994).

[4]P. Hamm, M. Lim, and R. M. Hochstrassr, J. Phys. Chem. B, **102**, 6123 (1998).

[5]V. Pajcini and S. Asher, J. Am. Chem. Soc., **121**, 10942 (1999).

[6]R. Schweitzer-Stenner, G. Sieler, and H. Christansen, Asian. J. Phys., **7**, 287 (1998).

[7]X. G. Chen, S. A. Asher, R. Schweitzer-Stenner, N. G. Mirkin, and S. Krimm, J. Am. Chem. Soc., **117**, 2884 (1995).

[8]G. Sieler, R. Schweitzer-Stenner, J. S. W. Holtz, V. Pajcini, and S. A. Asher, J. Phys. Chem. B, **103**, 372 (1999).

[9]Y. Liu, A. M. A. Czarnecki, and Y. Ozaki, Appl.Surf.Sci., **48**, 1095 (1994).

[10]N. E. Triggs and J. J. Valentini, J. Phys. Chem., **96**, 6922 (1992).

[11]G. Sieler and R. Schweitzer-Stenner, J. Am. Chem. Soc., **119**, 1720 (1997).

[12]R. Schweitzer-Stenner, G. Sieler, N. Mirkin, and S. Krimm, J. Phys. Chem. A, **102**, 118 (1998).

[13]S. Ataka, H. Takeuci, and M. Tasumi, J. Mol. Struct., **113**, 147 (1984).

[14]R. Ludwig, O. Reis, R. Winter, F. Weinhold, and T. C. Farrar, J. Phys. Chem. B, **102**, 9312 (1998).

[15]N. G. Mirkin and S. Krimm, J. Am. Chem. Soc., **112**, 9016 (1990).

[16]N. G. Mirkin and S. Krimm, Theochem. J. Molec. Struct., **236**, 97 (1991).

[17]L. M. Markham and B. S. Hudson, J. Phys. Chem., **100**, 2731 (1996).

[18]J. R. Maple, M.-J. Hwang, K. J. Jalkanen, T. P. Stockfisch, and A. T. Hagler, J. Comp. Chem., **19**, 430 (1998).

[19]S. W. Rick and B. J. Berne, J. Am. Chem. Soc., **118**, 672 (1996).

[20]N. A. Besley and J. D. Hirst, J. Phys. Chem. A, **102**, 10791 (1998).

[21]H. Torii, T. Tatsumi, and M. Tasumi, J. Raman Spectrosc., **29** (1998).

[22]N. G. Mirkin and S. Krimm, J. Am. Chem. Soc., **113**, 9742 (1991).

[23]F. Huisken, O. Werhahn, A. Y. Ivanov, and S. A. Krasnokutski, J. Chem. Phys., **111**, 2978 (1999).

[24]S. Davis, D. Uy, and D. Nesbitt, J. Chem. Phys., **112**, 1823 (2000).

[25]D. Uy, S. Davis, and D. Nesbitt, J. Chem. Phys., **109**, 7793 (1998).

[26]O. Votava, J. D. Fair, D. F. Plusquellic, and E. Riedle D. J. Nesbitt, J. Chem. Phys., **107**, 8854 (1997).

[27]D. T. Anderson, S. Davis, and D. J. Nesbitt, J. Chem. Phys., **107**, 1115 (1997).

[28]J. A. Dickinson, M. R. Hockridge, R. T. Kroemer, E. G. Robertson, and J. P. Simons, J. Am. Chem. Soc., **180**, 2622 (1998).

[29]M. R. Hockridge, E. G. Robertson, and J. P. Simons, Chem. Phys. Lett., **302**, 538 (1999).

[30]K. Naura and R. E. Miller, Science, **287**, 293 (2000).

[31]K. Naura, D. T. Moore, and R. E. Miller, Faraday Discuss. Chem. Soc., **113**, 261 (2000).

[32]A. Lindinger, J. P. Toennies, and A. F. Vilesov, J. Chem. Phys., **110**, 1429 (1998).

[33]M. C. Asplund, M. T. Zanni, and R. M. Hochstrassr, Proc. Nat. Acad. Sci., **97**, 8219 (2000).

[34]M. T. Zanni, M. C. Asplund, and R. M. Hochstrassr, J. Chem. Phys., **114**, 4579 (2001).

[35]P. Hamm, M. Lim, M. Asplund, and R. M. Hochstrassr, Proc. Nat. Acad. Sci., **96**, 2036 (1999).

[36]P. Hamm, M. Lim, M. Asplund, and R. M. Hochstrassr, Chem. Phys. Lett., **301**, 167 (1999).

[37]W. M. Zhang, V. Chernyak, and S. Mukamel, J. Chem. Phys., **110**, 5011 (1999).

[38]S. Woutersen and P. Hamm, J. Phys. Chem. B, **104**, 11316 (2000).

[39]J. O. Jung and R. B. Gerber, J. Chem. Phys., **105**, 10682 (1996).

[40]S. K. Gregurick, E. Fredj, R. Elber, and R. B. Gerber, J. Phys. Chem., **101**, 8595 (1997).

[41]S. K. Gregurick, J. H.-Y. Liu, D. A. Brant, and R. B. Gerber, J. Phys. Chem., **103**, 3476 (1999).

[42]A. Roitberg, R. B. Gerber, R. Elber, and M. A. Ratner, Science, **268**, 1319 (1995).

[43]G. M. Chaban, J. O. Jung, and R. B. Gerber, J. Chem. Phys., **111**, 1823 (1999).

[44]G. M. Chaban, J. O. Jung, and R. B. Gerber, J. Phys. Chem. A, **104**, 2772 (2000).

[45]G. M. Chaban, J. 0. Jung, and R. B. Gerber, J. Phys. Chem. A, **104**, 10035 (2000).

[46]G. M. Chaban and R. B. Gerber, J. Chem. Phys. (2001), in press.

[47]R. B. Gerber and M. A. Ratner, Adv. Chem. Phys., **70**, 97 (1988).

[48]J. M. Bowman, J. Chem. Phys., **68**, 608 (1978).

[49]R. B. Gerber and M. A. Ratner, Chem. Phys. Lett., **68**, 195 (1979).

[50]J. M. Bowman, Acc. Chem. Res., **19**, 202 (1986).

[51]W. D. Cornell, P. Cieplak, C. I. Bayly, I. R. Gould, K. M. Merz Jr., D. M. Ferguson, D. C. Spellmeyer, T. Fox, J. W. Caldwell, and P. A. Kollman, J. Am. Chem. Soc., **117**, 5179 (1995).

[52]H. H. Nielsen, Rev. Mod. Phys., **23**, 90 (1951).

[53]W. Schneider and W. Thiel, Chem. Phys. Lett., **157**, 367 (1989).

[54]J. O. Jung and R. B. Gerber, J. Chem. Phys., **105**, 10332 (1996).

[55]W. Yang and A. C. Peet, Chem. Phys. Lett., **153**, 98 (1988).

[56]M. W. Schmidt, K. K. Baldridge, J. A. Boatz, S. T. Elbert, M. S. Gordon, J. H. Jensen, N. Matsunaga, K. A. Nguyet adn S. Sa, T. L. Windus, M. Dupuis, and J. A. Montgomery, J. Comp. Chem., **14**, 1347 (1993).

[57]T. H. Dunning and P. J. Hay, *Methods of Electronic Structure Thoery*, (Plenum, New York, 1977).

[58]N. J. Wright and R. B. Gerber, J. Chem. Phys., **112**, 2598 (2000).

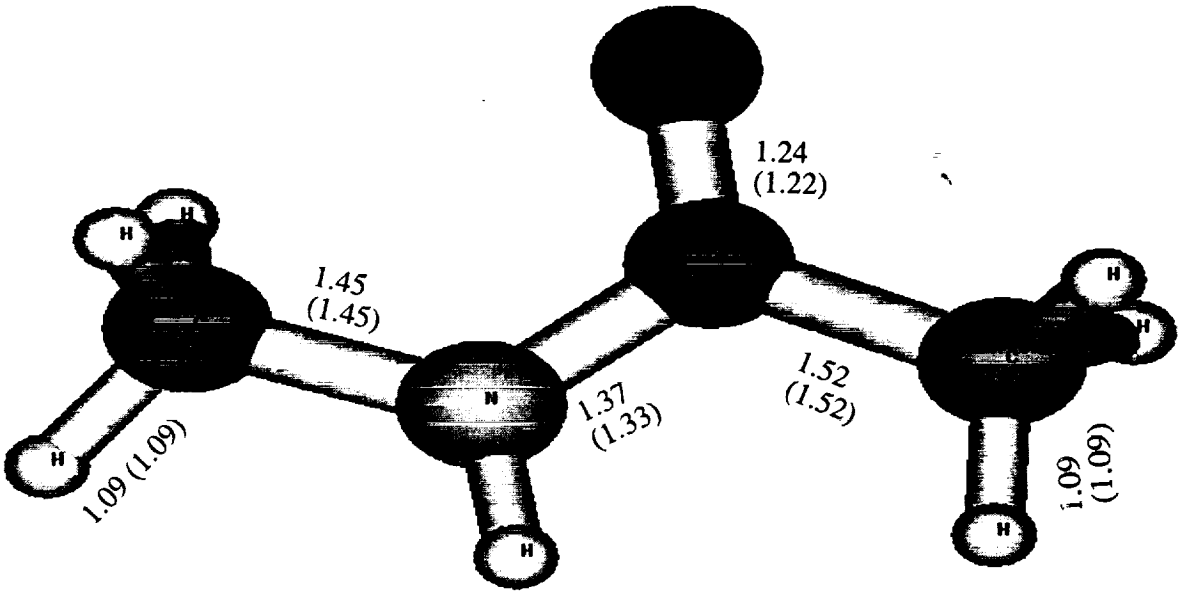

CNC Angle 120.7 (121.95)
NCC Angle 115 (117)

CNCO Torsion –3.62 (0.08)
HNCO Torsion –173.34 (–179.9)

Figure 1: The optimized equilibrium structure of *trans*-N-Methylacetamide. Bond lengths (in Å) and angles (in degrees) are given for the *ab initio* MP2/DZP and empirical (parenthesis) optimized structure of NMA.

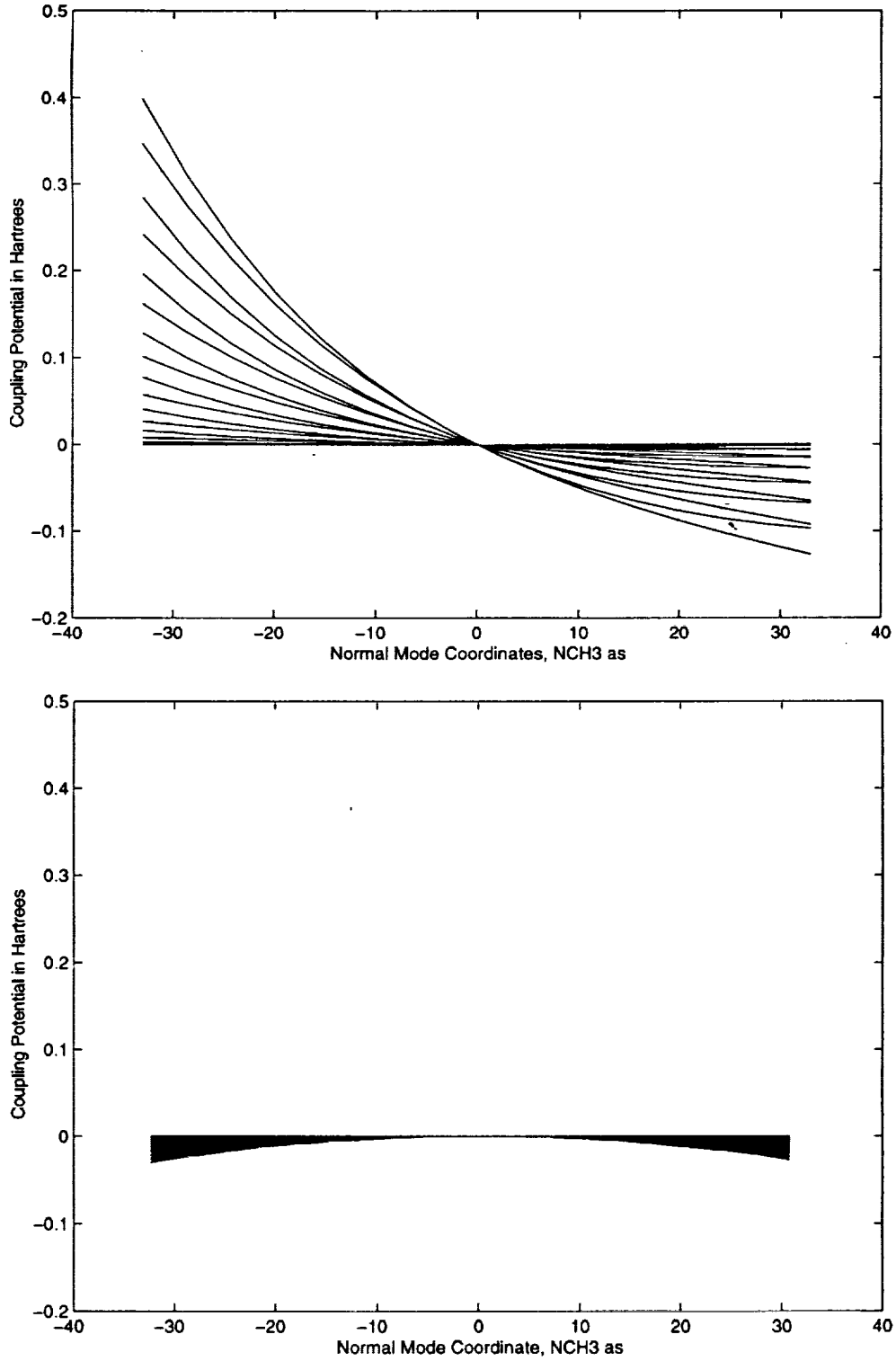

Figure 2: The coupling potential between the NCH_3 asymmetric stretch and the CH_3 asymmetric stretch (modes 2 and 5) for the *ab initio* (top panel) and the empirical (bottom panel) force fields. The normal mode coordinates are in a dimensionless variable as given by equation 2.A.3. The coupling potential is given in Hartrees. For comparison the potentials are given on the same scale.

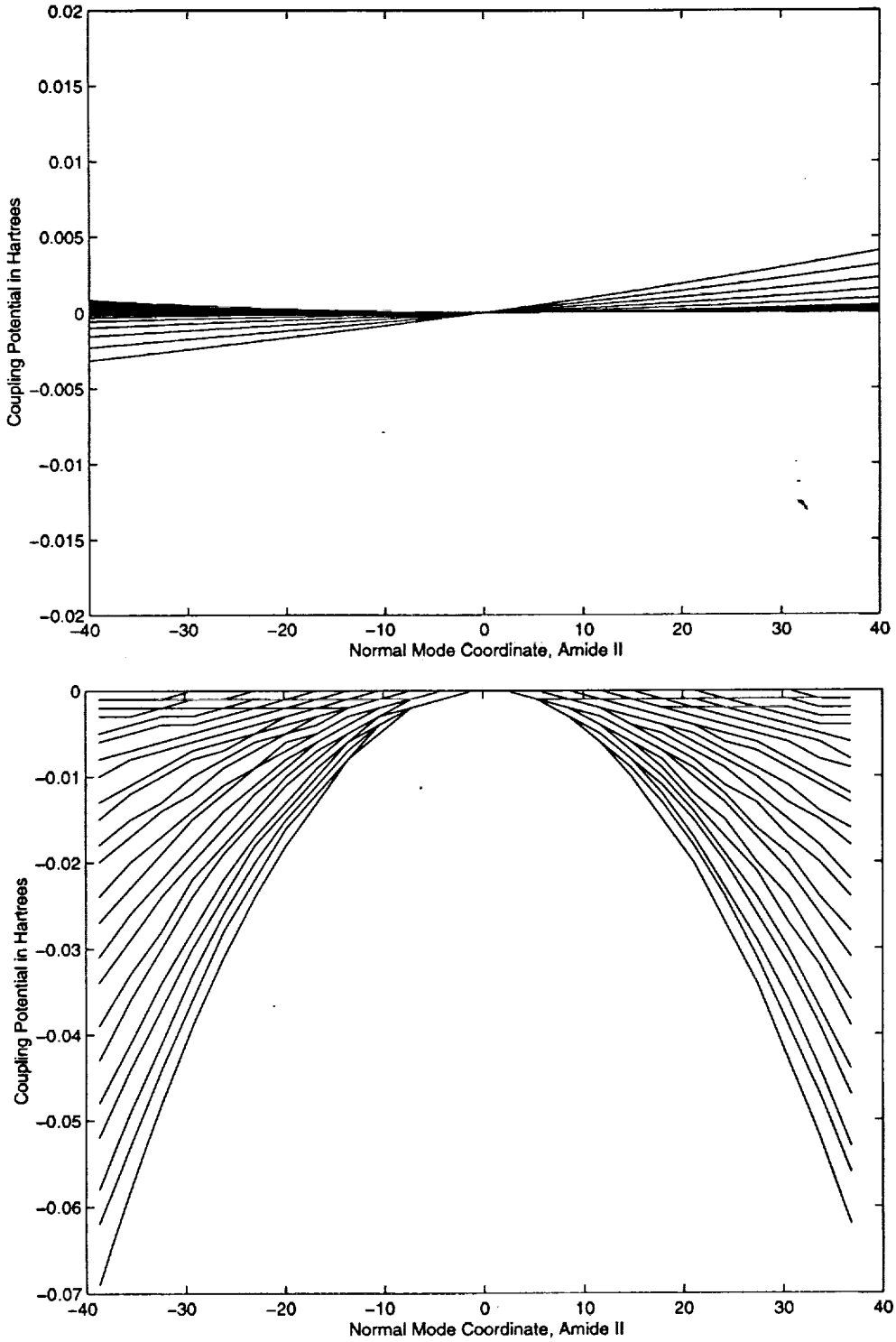

Figure 3: The coupling potential between the amide II and the CH_3 ab (modes 9 and 11) for the *ab initio* (top panel) and the empirical (bottom panel) force fields. The normal mode coordinates are in a dimensionless variable as given by equation 2.A.3. The coupling potential is given in Hartrees. For comparison the potentials are given on the same scale.

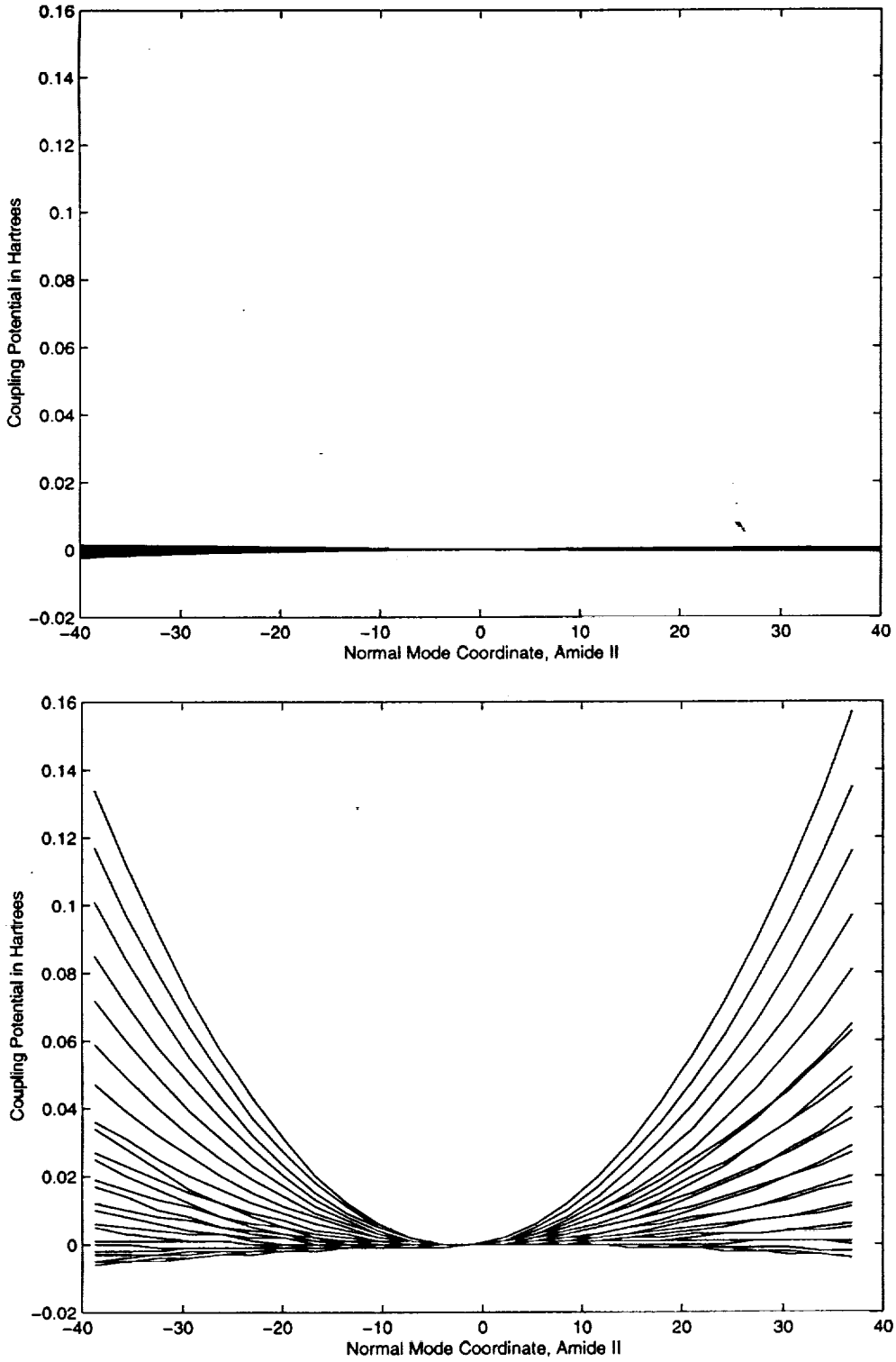

Figure 4: The coupling coupling potential between the Amide II and the NCH_3 sb NC s (modes 9 and 14) for the *ab initio* (top panel) and the empirical (bottom panel) force fields. The normal mode coordinates are in a dimensionless variable as given by equation 2.A.3. The coupling potential is given in Hartrees.

Table 4: Coupling Strength for the Adjusted Empirical Force Field

	1	2	3	4	5	6	7	8	9	10	11	12	13	14	15	16	17	18	19	20	21	22	23	24	25	26	26	28	29	30
1	0	0.0	0.0	0.0	0.0	0.0	0.0	0.0	0.0	0.0	0.0	0.0	0.0	0.0	0.0	0.0	0.0	0.0	0.0	0.0	0.0	0.0	0.0	0.0	0.0	0.0	0.0	0.0	0.0	0.0
2		0	0.0	0	0.0	0	0.0	0.0	0.0	0.0	0.0	0.0	0.0	0.0	0.0	0.0	0.0	0.0	0.0	0.0	0.0	0.0	0.0	0.0	0.0	0.0	0.0	0.0	0.0	0.0
3			0	0.0	0.0	0.3	0.0	0.0	0.0	0.0	0.0	0.0	0.0	0.0	0.0	0.0	0.1	0.0	0.0	0.0	0.0	0.0	0.0	0.0	0.0	0.0	0.0	0.0	0.0	0.0
4				0	0.0	0.0	0.2	0.0	0.0	0.0	0.0	0.0	0.0	0.0	0.0	0.0	0.2	0.0	0.0	0.0	0.0	0.0	0.0	0.0	0.0	0.0	0.0	0.0	0.0	0.0
5					0	0.0	0.0	0.0	0.0	0.0	0.0	0.0	0.0	0.0	0.0	0.0	0.0	0.0	0.0	0.0	0.0	0.0	0.0	0.0	0.0	0.0	0.0	0.0	0.0	0.0
6						0	0.0	0.0	0.0	0.0	0.0	0.0	0.0	0.0	0.0	0.0	0.0	0.0	0.0	0.0	0.0	0.0	0.0	0.0	0.0	0.0	0.0	0.0	0.0	0.0
7							0	0.0	0.0	0.0	0.0	0.0	0.0	0.0	0.0	0.0	0.0	0.0	0.0	0.0	0.0	0.0	0.0	0.0	0.0	0.0	0.0	0.0	0.0	0.0
8								0	0.0	0.0	0.0	0.0	0.0	0.0	0.0	0.0	0.0	0.0	0.0	0.0	0.0	0.0	0.0	0.0	0.0	0.0	0.0	0.0	0.0	0.0
9									0	1.8	-0.1	0.0	0.0	-0.2	0.0	0.0	0.0	0.0	-0.6	0.0	0.1	0.0	0.0	0.0	0.0	0.0	0.0	0.0	0.0	0.0
10										0	-5.4	0.0	0.0	0.0	0.0	0.0	0.0	8.5	0.0	0.1	0.0	0.0	0.0	0.0	0.0	0.0	0.0	0.0	0.0	0.0
11											0	7.4	0.0	0.0	1.4	0.0	-1.0	1.2	0.7	0.2	0.0	0.0	0.0	0.0	0.0	0.0	0.0	0.0	0.0	0.0
12												0	10.2	0.0	0.0	0.2	0.7	0.0	0.7	0.3	0.0	0.0	0.0	0.0	0.0	0.0	0.0	0.0	0.0	0.0
13													0	0.0	-0.5	0.0	0.3	0.8	0.7	0.0	0.0	0.0	0.0	0.0	0.0	0.0	0.0	0.0	0.0	0.0
14														0	-14.0	0.2	0.6	-0.2	2.3	1.2	0.0	0.1	0.0	0.0	0.0	0.0	0.0	0.0	0.0	0.0
15															0	4.9	1.1	1.5	-0.1	0.0	0.0	0.0	0.0	0.0	0.0	0.0	0.0	0.0	0.0	0.0
16																0	0.9	3.5	0.0	0.2	0.6	0.0	0.2	0.0	0.0	0.0	0.0	0.0	0.0	0.0
17																	0	0.9	3.8	11.4	0.1	0.0	0.0	0.0	0.0	0.0	0.0	0.0	0.0	0.0
18																		0	20.3	0.3	0.9	0.0	0.0	0.0	0.0	0.0	0.0	0.0	0.3	0.0
19																			0	18.4	1.5	3.4	0.1	0.5	0.0	0.0	0.0	0.0	0.3	0.3
20																				0	5.8	5.3	0.0	0.3	0.0	0.0	0.0	0.0	0.3	0.2
21																					0	-3.6	-0.1	0.0	0.0	0.0	0.0	0.0	0.0	-0.1
22																						0	-0.1	0.0	0.0	0.0	0.0	0.0	-0.2	0.0
23																							0	0.0	0.0	0.0	0.0	0.0	0.0	0.0
24																								0	0.0	0.0	0.0	0.0	0.0	0.1
25																									0	0.0	0.0	0.0	0.0	0.0
26																										0	0.0	0.0	0.0	0.0
27																											0	0.2	0.0	0.0
28																												0	0.0	0.0
29																													0	-1.9

Table 5: Coupling Strength for the *Ab Initio* Force Field

	1	2	3	4	5	6	7	8	9	10	11	12	13	14	15	16	17	18	19	20	21	22	23	24	25	26	26	28	29	30
1	0	0.0	0.0	0.0	0.0	0.0	0.0	0.0	0.0	0.0	0.0	0.0	0.0	0.0	0.0	0.0	0.0	0.0	0.0	0.0	0.0	0.0	0.0	0.0	0.0	-0.1	0.0	0.0	0.0	0.0
2		0	0.0	0.0	4.1	0.0	1.4	0.0	0.0	0.0	0.0	0.0	0.0	0.0	0.0	0.0	0.0	0.0	0.0	0.0	0.0	0.0	0.0	0.0	0.0	0.0	0.0	0.0	0.0	-0.1
3			0	-1.2	0.0	1.3	0.0	0.0	0.0	0.0	0.0	0.0	0.0	0.0	0.0	0.0	0.0	0.0	0.0	0.0	0.0	0.0	0.0	0.0	0.0	0.0	0.0	0.0	-0.1	0.0
4				0	0.0	0.9	0.0	0.0	0.0	0.0	0.0	0.0	0.0	0.0	0.0	0.0	0.0	0.0	0.0	0.0	0.0	0.0	0.0	0.0	0.0	0.0	0.0	0.0	0.0	0.0
5					0	0.0	2.4	0.0	0.0	0.0	0.0	0.0	0.0	0.0	0.0	0.0	0.0	0.0	0.0	0.0	0.0	0.0	0.0	0.0	0.0	0.0	0.0	0.0	0.0	-0.1
6						0	-0.9	0.0	0.0	0.0	0.0	0.0	0.0	0.0	0.0	0.0	0.0	0.0	0.0	0.0	0.0	0.0	0.0	0.0	0.0	0.0	0.0	0.0	0.0	0.0
7							0	0.0	0.0	0.0	0.0	0.0	0.0	0.0	0.0	0.0	0.0	0.0	0.0	0.0	0.0	0.0	0.0	0.0	0.0	0.0	0.0	0.0	0.0	-0.1
8								0	0.0	0.0	0.0	0.0	0.0	0.0	0.0	0.0	0.0	0.0	0.0	0.0	0.0	0.0	0.0	0.0	0.0	0.0	0.0	0.0	0.0	0.0
9									0	-0.1	0.2	0.0	0.0	0.0	0.0	0.0	0.0	0.0	0.0	0.0	0.0	0.0	0.0	0.0	0.0	0.0	0.0	0.0	0.0	0.0
10										0	0.0	-0.1	0.0	0.0	0.0	0.0	0.0	0.0	0.0	0.0	0.0	0.0	0.0	0.0	0.0	0.0	0.0	0.0	0.0	0.1
11											0	0.0	0.0	0.0	0.0	0.0	0.0	0.0	0.0	0.0	0.0	0.0	0.0	0.0	0.0	0.0	0.0	0.0	0.0	0.0
12												0	0.0	0.0	0.0	0.0	0.0	0.0	0.0	0.0	0.0	0.0	0.0	0.0	0.0	0.0	0.0	0.0	0.0	0.1
13													0	0.0	0.0	0.0	0.0	0.0	0.0	0.0	0.0	0.0	0.0	0.0	0.0	0.0	0.0	0.0	0.0	0.0
14														0	0.0	0.0	0.0	0.0	0.0	0.0	0.0	0.0	0.0	0.0	0.0	0.0	0.0	0.0	0.0	0.0
15															0	0.0	0.0	0.0	0.0	0.0	0.0	0.0	0.0	0.0	0.0	0.0	0.0	0.0	0.0	0.0
16																0	0.0	0.0	0.0	0.0	0.0	0.0	0.0	0.0	0.0	0.0	0.0	0.0	0.0	0.0
17																	0	0.0	0.0	0.0	0.0	0.0	0.0	0.0	0.0	0.0	0.0	0.0	0.0	0.1
18																		0	0.0	0.0	0.0	0.0	0.0	0.0	0.0	0.0	0.0	0.0	0.0	0.1
19																			0	0.0	0.0	0.0	0.0	0.0	0.0	0.0	0.0	0.0	0.0	0.0
20																				0	0.0	0.0	0.0	0.0	0.0	0.0	0.0	0.0	0.1	0.0
21																					0	0.0	0.0	0.0	0.0	0.0	0.0	0.0	0.0	0.0
22																						0	0.0	0.0	0.0	0.0	0.0	0.0	0.0	0.0
23																							0	1.1	0.0	0.1	0.0	0.0	0.0	0.0
24																								0	0.0	0.1	0.0	0.0	0.0	0.0
25																									0	0.0	0.0	0.0	0.1	0.0
26																										0	0.0	0.2	0.0	0.0
27																											0	0.1	0.0	1.0
28																												0	0.4	-1.4
29																													0	0.0

Table : Enumeriation of Modes for *trans* N-Methylacetamide

mode number	assignment
1	NH stretch
2	NCH_3 as
3	CCH_3 as
4	CH_3 as
5	CH_3 as
6	NCH_3 ss
7	CCH_3 ss
8	amide I
9	amide II
10	NCH_3 asy bend (ab)
11	CH_3 ab
12	CCH_3 ab
13	NCH_3 ab
14	NCH_3 sb NC s
15	CCH_3 ab
16	amide III
17	NH opb, CH_3r CNs
18	CN s CH_3r
19	CO opb CCH_3r
20	CO opb CCH_3r
21	CH_3r CC s CO opb
22	amide V CH_3r
23	CH_3r CO ipb
24	CCs CO opb
25	amide IV CH_3r
26	CO opb CCH_3r
27	CNC d CCN d
28	CNC d CCN d CCH_3d
29	NCH_3 d
30	CCH_3 d

s=stretch, as=asymeteric stretch, ss=symmetric stretch, d=distortion, r=rocking,ab=asymmetric bend, sb=symmetric